NASA TECHNICAL NOTE

THE RESPONSES OF BALLOON AND FALLING SPHERE WIND SENSORS IN TURBULENT FLOWS

by George H. Fichtl

George C. Marshall Space Flight Center
Marshall Space Flight Center, Ala. 35812

NATIONAL AERONAUTICS AND SPACE ADMINISTRATION • WASHINGTON, D. C. • FEBRUARY 1971

1. Report No.	2. Government Accession No.	3. Recipient's Catalog No.
NASA TN D-7049		

4. Title and Subtitle

The Responses of Balloon and Falling Sphere Wind Sensors in Turbulent Flows

5. Report Date: February 1971

6. Performing Organization Code

7. Author(s)

George H. Fichtl

8. Performing Organization Report No.: M166

9. Performing Organization Name and Address

George C. Marshall Space Flight Center
Marshall Space Flight Center, Alabama 35812

10. Work Unit No.

11. Contract or Grant No.

12. Sponsoring Agency Name and Address

National Aeronautics and Space Administration
Washington, D. C.

13. Type of Report and Period Covered: Technical Note

14. Sponsoring Agency Code

15. Supplementary Notes

Prepared by Aero-Astrodynamics Laboratory, Science and Engineering Directorate

16. Abstract

The responses of balloon and falling sphere wind sensors in turbulent flows are analyzed using Fourier transform techniques. The linearized equations of motion of a sensor that is subject to drag and gravitational body forces are developed by perturbing a sensor about an equilibrium uniform motion with turbulent or random wind fluctuations. The wind environment and sensor velocities are decomposed with stochastic Fourier-Stieltjes integrals, and the linearized equations of motion are used to derive the response functions and phase angles of the sensor motions. The results of the analysis are used to analyze the response properties of the Jimsphere balloon wind sensor and the effects that balloon motions would have on turbulence spectra if they were calculated with ballon and falling sphere wind data.

The Kolmogorov inertial subrange and the Lumley subrange for nearly inertial isotropic turbulence in stably stratified fluids are used as specific examples in the calculations.

17. Key Words (Suggested by Author(s))

Balloon Response
Falling Sphere Response
Atmospheric Turbulence

18. Distribution Statement

19. Security Classif. (of this report)	20. Security Classif. (of this page)	21. No. of Pages	22. Price*
Unclassified	Unclassified	35	$3.00

*For sale by the National Technical Information Service, Springfield, Virginia 22151

TABLE OF CONTENTS

LIST OF ILLUSTRATIONS

LIST OF SYMBOLS

English Symbols

A	Cross-sectional area of sensor
C	Universal constant in the spectrum for the Lumley subrange
C_D	Drag coefficient
$dZ(\omega)$	Fourier amplitude
D	Diameter of sensor
g	Acceleration of gravity
$\vec{i}, \vec{j}$	Horizontal, orthogonal unit vectors
i	$\sqrt{-1}$
I'	Integral of the sensor vertical velocity
k	m_a/m_o, dimensionless, experimentally determined parameter
$\vec{k}$	Vertical unit vector
m	Mass of the sensor
m_a	Apparent mass of sensor
m_g	Mass of sensor gas
m_o	Mass of air displaced by sensor
M_g	Molecular weight of sensor gas
M_o	Molecular weight of air
p	Exponent in power law spectra
Re	Reynolds number
t	Time

LIST OF SYMBOLS (Continued)

English Symbols (Concluded)

T	Time constant
T_o	Temperature of an adiabatic atmosphere
u, v	Horizontal, orthogonal components of the sensor velocity vector
u_e, v_e	Horizontal, orthogonal components of the environmental velocity vector
$\vec{V}$	Velocity vector of sensor
$\vec{V}_e$	Environmental velocity vector
w	Vertical velocity of sensor
w_e	Vertical environmental velocity
z	Altitude

Greek Symbols

α	$m_a/(m + m_a)$
α_1	Universal constant in the spectrum for Kolmogorov subrange
β	Power spectrum parameter
δ	Phase angle
ϵ	Viscous dissipation
$\bar{\theta}$	Mean flow potential temperature
κ	Wave number (rad m^{-1})
λ	Vertical wavelength
ν	Coefficient of kinematic viscosity of air

LIST OF SYMBOLS (Concluded)

Greek Symbols (Concluded)

ρ	Atmospheric density
ϕ	Power spectrum in frequency domain
Φ	Power spectrum in wave number domain
ψ	Dimensionless spectrum
ω	Frequency (rad sec^{-1})

Miscellaneous Symbols

$( )'$	Perturbation quantity
$\overline{( )}$	Basic state quantity
$\| \|$	Absolute value
$< >$	Ensemble average
d/dt	Differentiation with respect to t

THE RESPONSES OF BALLOON AND FALLING SPHERE WIND SENSORS IN TURBULENT FLOWS

SUMMARY

The responses of balloon and falling sphere wind sensors in turbulent and random flows are analyzed in this report. The basic equations of motion appropriate for a sensor influenced by drag and buoyant forces are linearized by perturbing an equilibrium uniform motion of a sensor with turbulent or random wind fluctuations. The wind environment and sensor velocities are decomposed with stochastic Fourier-Stieltjes integrals. Substitution of these representations into the linearized equations of motion yields the response of the wind sensor. The response functions in turn yield the transfer functions of the sensor and the phase angles of the Fourier components of the balloon motion. The transfer functions and phase angles are functions of the wind perturbation frequency ω and contain two parameters T and a which are functions of sensor mass, apparent mass of the sensor, the mass of air displaced by the sensor, the ascent or descent rate of the sensor as the case may be, and the acceleration of gravity. The quantity T is a time constant of the system and a is the ratio of the apparent mass to the sum of the apparent mass and the mass of the system. Once these quantities are specified, the response properties of the sensor are completely specified in a linear context. In general the system becomes more responsive as T and a approach zero and unity respectively.

As $\omega T \to 0$, the transfer functions and phase angles approach unity and zero, respectively; so that at sufficiently low frequencies, the sensor essentially measures 100 percent of the turbulent Fourier amplitudes with no phase shifts. As $\omega T \to \infty$, the transfer functions and phase angles approach a^2 and zero, respectively; so that at sufficiently large frequencies, the sensor is capable of detecting a percentage (equal to $100a$) of the turbulent Fourier amplitudes, again with no phase shifts. If apparent mass effects were not present ($a = 0$), the sensor transfer functions would approach zero as $\omega T \to \infty$. Thus, the apparent mass effects make the sensor more responsive. At $\omega T = a^{-1/2}$ for the horizontal fluctuations and $\omega T = 2\, a^{-1/2}$ for the vertical velocity fluctuations, the phase angles of the sensor Fourier amplitudes take on minimum values. In general the transfer functions associated with the horizontal sensor motions are smaller than the transfer function associated with the vertical sensor motions in the domain $0 < \omega T < \infty$, and thus the sensor is more responsive to vertical air motions than to horizontal air motions.

The results of the analysis are used to analyze the response properties of the Jimsphere balloon wind sensor and the effects that balloon motions would have on turbulence spectra if they were calculated with balloon and falling sphere wind data. The Kolmogorov inertial subrange and the Lumley subrange in nearly inertial isotropic turbulence in stably stratified fluids are used as specific examples in the calculations.

INTRODUCTION

The subject of this paper is the responses of balloons and falling sphere wind sensors to the wind environment. It has been suggested in various quarters of the meteorological and aerospace communities that it might be possible to detect clear air turbulence and gravity wave phenomena with these devices, which include the Jimsphere spherical balloon [1], the ROSE balloon [2], and the ROBIN falling sphere [3]. To determine the capabilities of such devices with respect to measuring small vertical scale wind fluctuations, it is necessary to first determine their response properties. The responses of ballons and falling sphere wind sensors have been the subject of a number of investigations during the last decade [4-7]. However, these investigations have been concerned with the responses of these wind sensors to vertical variations of the horizontal wind. It now appears that it might be possible to detect vertical velocity fluctuations with these devices, at least with the Jimsphere [8]. Accordingly, the subject of this analysis is the responses of these devices to vertical variations of both the horizontal and vertical components of the wind as they traverse the wind field. The analysis will be based on linear perturbation theory, whereby the wind field is assumed to be composed of a constant basic state mean flow with a superimposed perturbation. Similarly, it is assumed that the associated velocity components of the wind sensor can also be represented in terms of a mean state and a superimposed perturbation. The perturbations are assumed to be sufficiently small, so that nonlinear terms in perturbation quantities can be neglected in comparison to first-order terms. This hypothesis results in a set of three linearized momentum conservation equations that govern the velocity perturbations of the sensor. The subsequent analyses of the response properties of the wind sensors are based on these equations. The Jimsphere is analyzed in detail as an example.

BASIC EQUATIONS

The basic equations of motion that govern the behavior of a wind sensor are given by

$$m \frac{du}{dt} = \frac{1}{2} \rho C_D A |\vec{V}_e - \vec{V}| (u_e - u) + m_a \frac{d}{dt} (u_e - u) \quad , \tag{1}$$

$$m \frac{dv}{dt} = \frac{1}{2} \rho C_D A |\vec{V}_e - \vec{V}| (v_e - v) + m_a \frac{d}{dt} (v_e - v) \quad , \tag{2}$$

and

$$m\frac{dw}{dt} = \frac{1}{2}\rho C_D A |\vec{V}_e - \vec{V}|(w_e - w) + m_a \frac{d}{dt}(w_e - w) - (m - m_o)g \quad , \qquad (3)$$

where m, m_a, A, and C_D denote the mass, apparent mass, cross-sectional area, and drag coefficient of the sensor, respectively; m_o is the mass of air displaced by the sensor; g is the acceleration of gravity; ρ is the density of the atmosphere; and t is time. The zonal, meridional, and vertical components of velocity of the sensor are u, v, and w, respectively; and the subscript e denotes the environmental wind components. The first term on the right side of each equation represents the associated component of the drag force. The drag force is assumed to act parallel and opposite to the direction of the wind vector relative to the sensor, $\vec{V}_e - \vec{V}$, where

$$\vec{V} = u\vec{i} + v\vec{j} + w\vec{k} \quad , \qquad (4)$$

$\vec{i}$, $\vec{j}$, and $\vec{k}$ being zonal, meridional, and vertical unit vectors, respectively. The second term on the right side of equations (1) through (3) represents the effects of the sensor apparent mass [4]. The third term on the right side of equation (3) denotes the buoyant force.

The aerodynamic lift forces have been neglected in these equations. The effects of these forces on the sensor motion will be considered in a later report.

FIRST-ORDER LINEAR PERTURBATION EQUATIONS

The environmental wind is assumed to be composed of a constant basic horizontal flow with superimposed velocity fluctuations, so that

$$\left.\begin{aligned} u_e &= \bar{u}_e + u'_e(t) \\ v_e &= \bar{v}_e + v'_e(t) \\ w_e &= w'_e(t) \end{aligned}\right\} \quad , \qquad (5)$$

where the overbars and primes denote the basic state and fluctuating parts of the wind. It is assumed that the velocity components of the sensor can also be partitioned into two parts, as was the environmental wind, so that

$$\left.\begin{aligned} u &= \bar{u} + u'(t) \\ v &= \bar{v} + v'(t) \\ w &= \bar{w} + w'(t) \end{aligned}\right\} \quad . \tag{6}$$

The overbarred quantities represent a mean motion of the sensor, and the primed quantities denote the departures from the mean motion. It is now assumed that the basic-state quantities in equations (5) and (6) satisfy equations (1) through (3), and thus it is concluded that

$$\bar{u} = \bar{u}_e \quad , \tag{7}$$

$$\bar{v} = \bar{v}_e \quad , \tag{8}$$

$$\frac{1}{2} A \rho C_D |\bar{w}| \bar{w} = (m_o - m)g \quad . \tag{9}$$

These equations govern the mean motion of the sensor. Equations (7) and (8) state that the sensor follows the mean horizontal motion of the environment. This results because the horizontal basic-state accelerations of the sensor and the environment vanish. Equation (9) states that the vertical drag force balances the Archimedean and gravitational body forces. The quantity $\bar{w}$ is the mean ascent or descent rate of the sensor. If $m_o > m$, then $\bar{w} > 0$, which corresponds to an ascending sensor; and if $m_o < m$, then $\bar{w} < 0$, which corresponds to a descending sensor. An example of the former is the Jimsphere spherical balloon [1], while an example of the latter is the ROBIN falling sphere [3].

Substitution of equation (5) and equation (6) into equations (1) through (3) and utilization of equations (7) and (8) yield the equations that govern the perturbations (prime quantities) of the sensor about the unperturbed state, so that

$$m\frac{du'}{dt} = \frac{1}{2}\rho C_D A\left[(u'_e - u')^2 + (v'_e - v')^2 + (w'_e - \bar{w} - w')^2\right]^{1/2}(u'_e - u')$$

$$+ m_a \frac{d}{dt}(u'_e - u') \quad , \tag{10}$$

$$m\frac{dv'}{dt} = \frac{1}{2}\rho C_D A\left[(u'_e - u')^2 + (v'_e - v')^2 + (w'_e - \bar{w} - w')^2\right]^{1/2}(v'_e - v')$$

$$+ m_a \frac{d}{dt}(v'_e - v') \quad , \tag{11}$$

and

$$m\frac{dw'}{dt} = \frac{1}{2}\rho C_D A\left[(u'_e - u')^2 + (v'_e - v')^2 + (w'_e - \bar{w} - w')^2\right]^{1/2}(w'_e - \bar{w} - w')$$

$$+ m_a \frac{d}{dt}(w'_e - w') - (m - m_o)g \quad . \tag{12}$$

These equations can be simplified by assuming that the fluctuations of the environmental wind and the sensor components of velocity are infinitesimally small, so that products of perturbation quantities can be neglected in comparison to first-order quantities. Thus, for infinitesimal perturbations one has

$$m\frac{du'}{dt} = \frac{1}{2}\rho C_D A|\bar{w}|(u'_e - u') + m_a \frac{d}{dt}(u'_e - u') \quad , \tag{13}$$

$$m\frac{dv'}{dt} = \frac{1}{2}\rho C_D A|\bar{w}|(v'_e - v') + m_a \frac{d}{dt}(v'_e - v') \quad , \tag{14}$$

and

$$m\frac{dw'}{dt} = \rho C_D A|\bar{w}|(w'_e - w') + m_a \frac{d}{dt}(w'_e - w') \quad , \tag{15}$$

where equation (9) has been used in deriving equation (15). These equations state that the fluctuations u', v', and w' are the result of fluctuations in the drag force and the apparent mass terms. The effects resulting from the Archimedean and gravitational body forces are concentrated in the mean motion of the sensor [equation (9)]. Equations (13) and (14) are identical in form. This means that the zonal and meridional balloon responses are proportional to each other.

It should be noted that the environmental velocity fluctuations are being treated as functions of time. Actually the wind field is a function of space and time. As the sensor passes through the wind field, it responds to both the temporal and spatial variations of the wind field. Thus, the sensor yields neither a Lagrangian nor a Eulerian measurement. It shall be assumed that the time scale of the atmospheric motions are sufficiently large compared to the time it takes for the sensor to traverse a particular atmospheric layer, so that the temporal variations of the wind field can be neglected. In addition, it will be assumed that the horizontal variations of the atmospheric wind field are sufficiently large, so that the sensor is essentially responding to vertical variations of the wind field. Thus, in essence, the wind perturbations are assumed to be functions of z only. Now, the explicit time dependence of the wind perturbations indicated in equation (5) is with respect to the sensor, and results because the sensor is ascending through the wind field. To show that this is valid in a linear context, it is noted that the height coordinate z can be transformed to a time coordinate with

$$z = \bar{w}t + \int_0^t w'(\xi)\, d\xi \quad . \tag{16}$$

Now, $w'(t)$ is a fluctuating quantity, and the negative and positive contributions to the above integral would tend to cancel each other. This means that this integral will fluctuate in sign and, more importantly, will remain small. Now,

$$u'_e(z) = u'_e\left[\left(1 + \frac{I'}{\bar{w}t}\right)\bar{w}t\right] \quad , \tag{17}$$

where I' denotes the integral in equation (16). Upon expanding u'_e in a Maclaurin series about $I'/\bar{w}t = 0$, the following is found:

$$u'_e(z) = u'_e(\bar{w}t) + \left(\frac{du'_e}{dz}\right)_{z=\bar{w}t} I' + \ldots . \tag{18}$$

The lead term in this expansion is a linear quantity, and the remaining terms are of second and higher order of smallness; therefore to be within first order, one has

$$u'_e(z) = u'_e(\bar{w}t) \quad , \tag{19}$$

which proves that the environmental wind perturbations can be transformed into explicit functions of time by replacing z with $\bar{w}t$ in the linear problem where $\bar{w}$ is now assumed to be a known quantity. The transformation is not so simple in the nonlinear problem, because the balloon vertical velocity fluctuation w' is contained in the forcing function through the integral I'.

FOURIER DECOMPOSITION

Suppose that u'_e, v'_e, and w'_e are random functions of time, so that u, v, and w are also random functions of time. Random functions are neither periodic nor integrable, therefore neither Fourier series nor integrals may be used in the ordinary sense. Nevertheless, under a set of weak assumptions, a Fourier representation does exist. According to Lumley and Panofsky [9], the theorem states that the random functions u'(t), v'(t), and w'(t) can be expanded in terms of the random functions $Z_u(\omega)$, $Z_v(\omega)$, and $Z_w(\omega)$, so that

$$u'(t) = \int_{-\infty}^{\infty} e^{i\omega t}\, dZ_u(\omega) \quad , \tag{20}$$

$$v'(t) = \int_{-\infty}^{\infty} e^{i\omega t}\, dZ_v(\omega) \quad , \tag{21}$$

and

$$w'(t) = \int_{-\infty}^{\infty} e^{i\omega t}\, dZ_w(\omega) \quad . \tag{22}$$

Similarly, the environmental wind fluctuation components $u'_e(t)$, $v'_e(t)$, and $w'_e(t)$ can be expanded in terms of the random functions $Z_{u_e}(\omega)$, $Z_{v_e}(\omega)$, and $Z_{w_e}(\omega)$, so that

$$u'_e(t) = \int_{-\infty}^{\infty} e^{i\omega t}\, dZ_{u_e}(\omega) \quad , \tag{23}$$

$$v'_e(t) = \int_{-\infty}^{\infty} e^{i\omega t}\, dZ_{v_e}(\omega) \quad , \tag{24}$$

and

$$w'_e(t) = \int_{-\infty}^{\infty} e^{i\omega t}\, dZ_{w_e}(\omega) \quad . \tag{25}$$

The Fourier amplitude $dZ_u(\omega)$ is a complex function of ω and is given by

$$dZ_u(\omega) = \lim_{\tau\to\infty} \frac{1}{2\pi} \int_{-\tau}^{\tau} u'(t)\, e^{-i\omega t} \left(\frac{1 - e^{-itd\omega}}{it} \right) dt \quad . \tag{26}$$

Similar expressions can be written for the remaining random functions. Equation (26) is a Stochastic Fourier-Stieltjes integral. (See Reference 10 for an example.)

The equations that govern the Fourier amplitudes can be obtained by substituting equations (20) through (25) into equations (13) through (15) and noting that the functions $e^{i\omega t}$ constitute a complete orthogonal function set, so that

$$(1 + i\omega T)\, dZ_u(\omega) = (1 + ia\omega T)\, dZ_{u_e}(\omega) \quad , \tag{27}$$

$$(1 + i\omega T)\, dZ_v(\omega) = (1 + ia\omega T)\, dZ_{v_e}(\omega) \quad , \tag{28}$$

and

$$(2 + i\omega T)\, dZ_w(\omega) = (2 + ia\omega T)\, dZ_{w_e}(\omega) \quad , \tag{29}$$

where

$$T = \frac{(m + m_a)|\bar{w}|}{|m_o - m|\, g} \tag{30}$$

and

$$a = \frac{m_a}{m + m_a} \tag{31}$$

Division of equations (27) and (28) by $1 + i\omega T$ and equation (29) by $2 + i\omega T$ yields the Fourier amplitudes of the sensor motion, so that

$$dZ_u(\omega) = \frac{1 + ia\omega T}{1 + i\omega T} \, dZ_{u_e}(\omega) \quad , \tag{32}$$

$$dZ_v(\omega) = \frac{1 + ia\omega T}{1 + i\omega T} \, dZ_{v_e}(\omega) \quad , \tag{33}$$

and

$$dZ_w(\omega) = \frac{2 + ia\omega T}{2 + i\omega T} \, dZ_{w_e}(\omega) \quad . \tag{34}$$

Equations (32) through (34) give the Fourier amplitudes of the sensor velocity fluctuations as functions of ω, a, T and the Fourier amplitudes of the environmental wind fluctuations.

TRANSFER FUNCTIONS AND PHASE RELATIONSHIPS

The coefficients of $dZ_{u_e}(\omega)$, $dZ_{v_e}(\omega)$, and $dZ_{w_e}(\omega)$ in equations (32) through (34) are the system response functions and contain the phase and amplitude information of the sensor velocity fluctuations relative to the environmental wind fluctuations. The amplitude information can be obtained by multiplying each expression by its complex conjugate and then taking an ensemble average. For the zonal fluctuations, one has

$$\langle dZ_u(\omega)\, dZ_u^*(\omega) \rangle = \frac{1 + (a\omega T)^2}{1 + (\omega T)^2} \langle dZ_{u_e}(\omega)\, dZ_{u_e}^*(\omega) \rangle \quad , \tag{35}$$

where $\langle\rangle$ denotes an ensemble average and $(\,)^*$ denotes complex conjugation. The quantity $\langle dZ_u(\omega)\, dZ_u^*(\omega) \rangle$ is the contribution to the variance of u' for frequencies between ω and $\omega + d\omega$, so that

$$\langle dZ_u(\omega)\, dZ_u^*(\omega)\rangle = \phi_u(\omega)\, d\omega \quad , \tag{36}$$

where $\phi(\omega)$ is the spectrum of u'. Similar statements can be made about the remaining random functions. The following relationships between the various spectra follow from equations (32) through (34):

$$\frac{\phi_u(\omega)}{\phi_{u_e}(\omega)} = \frac{\phi_v(\omega)}{\phi_{v_e}(\omega)} = \frac{1 + (a\omega T)^2}{1 + (\omega T)^2} \tag{37}$$

and

$$\frac{\phi_w(\omega)}{\phi_{w_e}(\omega)} = \frac{4 + (a\omega T)^2}{4 + (\omega T)^2} \quad . \tag{38}$$

The quantities on the right side of these equations are the system transfer functions. As $\omega T \to 0$, the ratios between the sensor velocity spectra and the environmental spectra approach unity, so that the magnitudes of the Fourier amplitudes of the sensor approach the magnitudes of the Fourier amplitudes of the environmental wind fluctuations. As $\omega T \to \infty$, the ratios of equations (37) and (38) approach a^2. If the apparent mass terms were not present in equations (13) through (15), the system transfer functions would approach zero as $\omega T \to \infty$. Thus, the presence of the derivatives of the environmental wind fluctuations via the apparent mass terms result in the sensor being more responsive to the environment. It should be noted that $\phi_u(\omega)/\phi_{u_e}(\omega) < \phi_w(\omega)/\phi_{w_e}(\omega)$ for $\omega \neq 0$. This means that the sensor filters the horizontal environmental velocity fluctuations more than the vertical environmental velocity fluctuations, or, in other words, the sensor is more responsive to the vertical wind than to the horizontal wind.

The phase angles δ by which the sensor velocity Fourier amplitudes lag behind the environmental Fourier amplitudes can be obtained by calculating the arctangent functions of the ratios of the imaginary and real parts of the system response functions. Thus,

$$\delta_u = \delta_v = \tan^{-1}\left[\frac{(a - 1)\,\omega T}{1 + a\,(\omega T)^2}\right] \quad , \tag{39}$$

and

$$\delta_w = \tan^{-1}\left[\frac{2(a - 1)\,\omega T}{4 + a\,(\omega T)^2}\right] \quad . \tag{40}$$

The phase angles are negative because $a - 1 < 0$. As $\omega T \to 0$ and $\omega T \to \infty$, the arguments of the arctangent functions approach zero, and thus the phase angles approach zero. This means that at both sufficiently small and large frequencies, the sensor and environmental Fourier components are in phase. It follows that the phase angles experience minima at finite values of ωT. Upon differentiating equations (39) and (40) with respect to ωT and setting the resulting relationships equal to zero, one finds that δ_u and δ_w experience minima at

$$\left.\begin{aligned} (\omega T)_{\min,\,u} &= (\omega T)_{\min,\,v} = a^{1/2} \\ (\omega T)_{\min,\,w} &= 2\,a^{1/2} \end{aligned}\right\} \quad . \tag{41}$$

Thus, the minimum phase angle of the horizontal sensor velocity fluctuations occurs at one-half the frequency at which the vertical sensor velocity fluctuations have their minimum phase angle. If the apparent mass effects were not present ($a = 0$), the minimum phase angles would all equal 90 deg, and they would occur at infinitely large frequencies. Substitution of equation (41) into equations (39) and (40) will show that minimum phase angles of the horizontal and vertical sensor velocity fluctuations are equal and are given by

$$\delta_{u,\,\min} = \delta_{v,\,\min} = \delta_{w,\,\min} = \tan^{-1}\left(\frac{a-1}{2a^{1/2}}\right) \quad . \tag{42}$$

Thus, the minimum phase angles are functions of a only.

JIMSPHERE RESPONSE

It is instructive to consider a specific example in studies of this nature. In this section the transfer functions and phase angles associated with the Jimsphere wind sensor for standard atmospheric conditions will be calculated. The Jimsphere wind sensor is a spherical, 2-m diameter, 0.5-mil, metalized Mylar balloon, fabricated from 12 tailored gores. It has 398 protrusions (cones) approximately 0.08 m high. This sensor is a superpressurized device with two valves 180 deg apart to vent helium and thus maintain a superpressure approximately equal to 7 mb. This system has a ballast of 0.1 kg to reduce spurious motions, and the complete system, excluding the inflation gas, has a mass approximately equal to 0.408 kg.

According to Eckstrom [5] , the apparent mass m_a is related to the displaced air m_o through the relationship

$$m_a = k\, m_o \quad , \tag{43}$$

where k is a dimensionless, experimentally determined parameter. Eckstrom's experimental values for the Jimsphere ranged between 0.46 and 0.58 with an average or characteristic value equal to 0.51.

The total mass of the system is

$$m = m_g + m_s \quad , \tag{44}$$

where m_g and m_s denote the mass of the inflation gas (helium) and the mass of the Jimsphere. The quantity m_s equals 0.408 kg. The mass of the gas m_g can be calculated by assuming that the balloon is in thermal equilibrium with the environment and the excess pressure of the gas within the balloon (approximately 7 mb) with respect to the environment is negligible. Calculations by DeMandel and Krivo [8] show that departures from thermal equilibrium by as much as 10°C and the balloon overpressure produce only a 1.5-percent variation in the balloon rise rate w, so that the above assumptions appear reasonable. Thus, utilizing the ideal gas law, one has

$$\frac{m_g}{m_o} = \frac{M_g}{M_o} = \frac{4.0026 \text{ gm mole}^{-1}}{28.9644 \text{ gm mole}^{-1}} \quad , \tag{45}$$

where M_g and M_o denote the molecular weights of the sensor gas (helium) and the atmosphere. The radius of the Jimsphere is 1 m, and thus the mass of the displaced air is

$$m_o = \frac{4}{3}\, \pi \rho \quad . \tag{46}$$

Substitution of equations (43) through (46) into the expressions for a and T given by equations (30) and (31) yields

$$T = \frac{k + M_g M_o^{-1} + 3 m_s (4\pi\rho)^{-1}}{|1 - M_g M_o^{-1} - 3 m_s (4\pi\rho)^{-1}|} \frac{|\bar{w}|}{g} \tag{47}$$

and

$$a = \frac{k}{k + \frac{M_g}{M_o} + \frac{3 m_s}{4\pi\rho}} \tag{48}$$

Figure 1 gives T and a as functions of altitude calculated with equations (47) and (48). The computations of these curves were based on standard atmosphere values of ρ, the typical rise rates $\bar{w}$ of the Jimsphere balloon as determined by DeMandel and Krivo [8], and the above mentioned values for the remaining parameters. A typical rise rate of the Jimsphere in the troposphere is 5 m sec^{-1}. It is clear from Figure 1 that T is approximately equal to 0.5 sec in the first 8 km of the atmosphere. Above the 8-km level T increases rapidly. The quantity a is a monotonically decreasing function of altitude. The quantities a and T are clearly functions of altitude and depend on time through the transformation

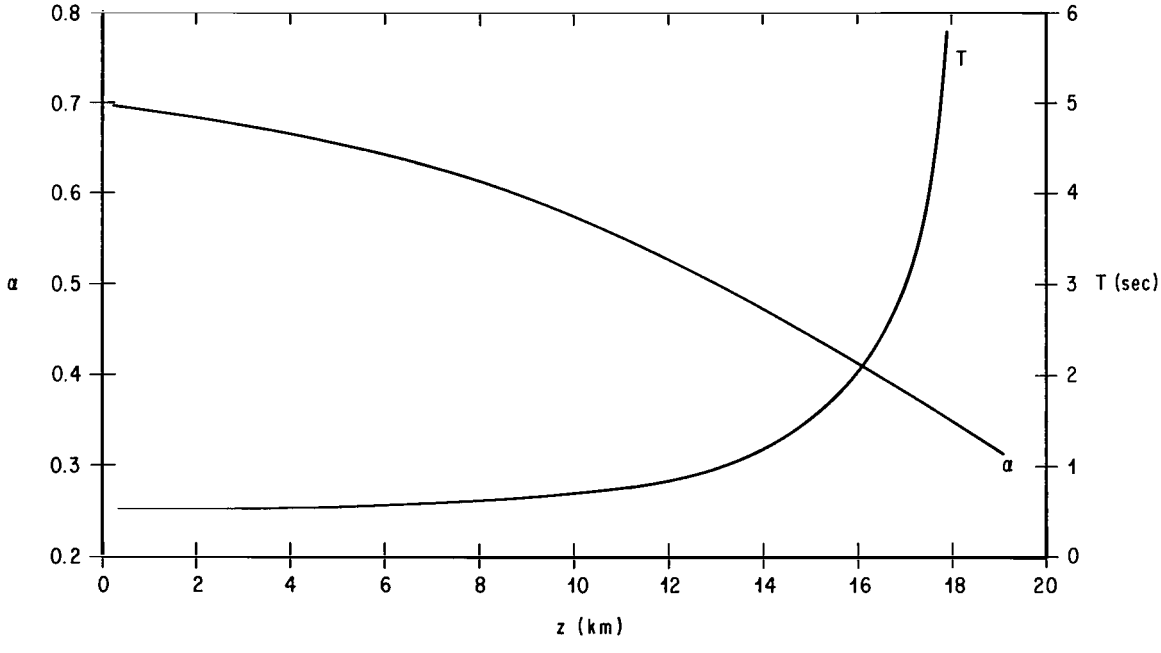

Figure 1. The quantities T and a as functions of altitude.

$z = \bar{w}t$. Thus, in the strictest sense, the perturbation equations (13) through (15) that govern the motion of the sensor are incorrect, because they were derived by assuming constant values for the balloon parameters (C_D, $\bar{w}$, etc.) and atmospheric density which means a and T were assumed to be constant. Nevertheless, it appears reasonable, as a first approximation, to apply the transfer functions and phase angle relationships locally at particular altitudes. The assumption here is that a and T do not vary appreciably over thin atmospheric layers with thicknesses that are large compared to the wavelengths of the atmospheric motions of concern. Past studies appear to show that the sensor velocity perturbations with wavelengths less than approximately 100 m are the ones that depart appreciably from the associated atmospheric perturbations [7]. The departure becomes more pronounced as the wavelength of the atmospheric perturbations becomes small. The quantities a and T have less than 10-percent vertical variation over a 1-km thick layer below approximately the 18-km and 13-km levels, respectively. Above the 13-km level, T has much larger vertical variation over a 1-km layer. Thus, for example, the quantity T has approximately a 30-percent vertical variation over a 1-km layer centered at the 17-km level. If 10-percent variations in a and T over a 1-km layer are accepted to be negligibly small, then it would appear that the analysis in this report could be applied over 1-km thick layers below the 13-km level, because the wavelengths of interest are less than or equal to approximately 10 percent of the layer thickness (1 km). Application of the analysis above the 13-km level will only lead to very approximate results. Nevertheless, the theory could be applied to levels above the 13-km level to obtain qualitative results.

Figures 2 through 5 are plots of the system transfer functions and the phase angles for $a = 0.7, 0.6, 0.5$, and 0.4. For the Jimsphere balloon, these values of a occur at approximately the surface and at the 8.5-, 13-, and 16.5-km levels, respectively. The figures show that as a decreases or as height increases, the magnitude of the minimum phase angles increases. The minima occur at $\omega T = a^{-1/2}$ and $2\,a^{-1/2}$ for the horizontal and vertical wind perturbations, respectively [equation (41)]. As a decreases or as height increases, the locations of the minima shift toward larger values of ωT. However T increases faster than $a^{1/2}$ decreases with height (Fig. 1), and thus, the minima actually shift toward smaller values of ω as height increases. This is clearly shown in Figure 6, a plot of the frequencies $\omega_{\min,\,u,\,v,\,w}$, at which the minimum phase angles occur as functions of altitude for the horizontal and vertical velocity perturbations of the Jimsphere. The wavelengths at which these minima occur are related to the rise rate through the expression,

$$\lambda_{\min} = \frac{2\pi\bar{w}}{\omega_{\min}} \quad . \tag{49}$$

Thus, for example, in the troposphere ($z \lesssim 10$ km) $\bar{w} \simeq 5$ msec^{-1}, $\omega_{\min,\,w} \simeq 4.4$ rad sec^{-1}, and $\omega_{\min,\,u} = \omega_{\min,\,v} = 2.2$ rad sec^{-1}. Substitution of these numbers into equation (49) yields the corresponding wavelengths $\lambda_{\min,\,w} \simeq 7$ m and $\lambda_{\min,\,u} = \lambda_{\min,\,v} \simeq 14$ m.

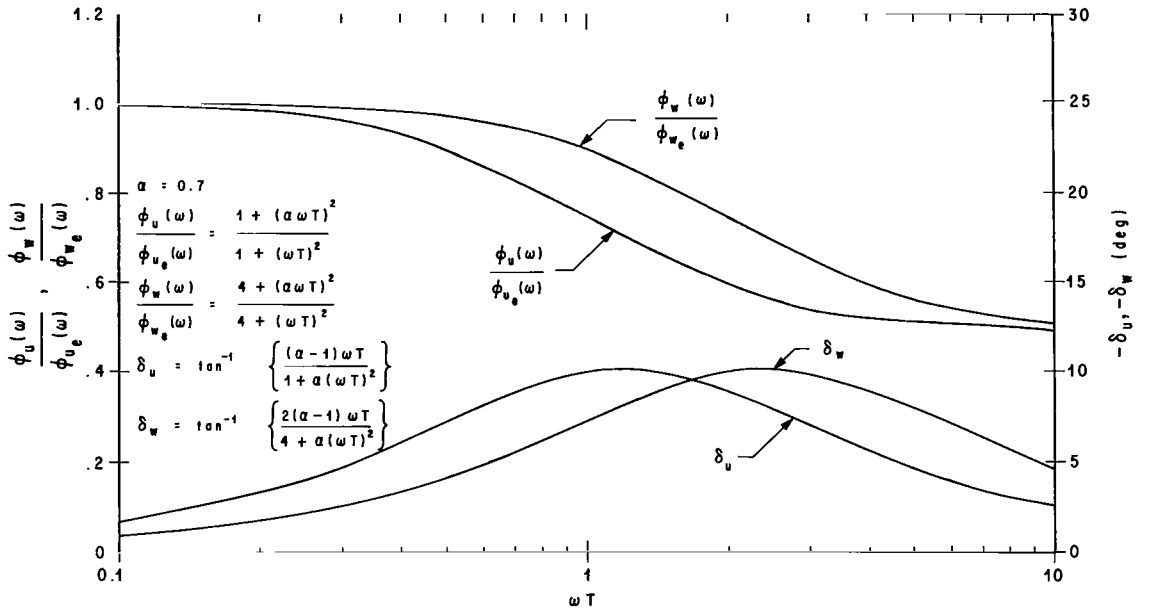

Figure 2. System transfer functions and phase angles as functions of ωT for $a = 0.7$.

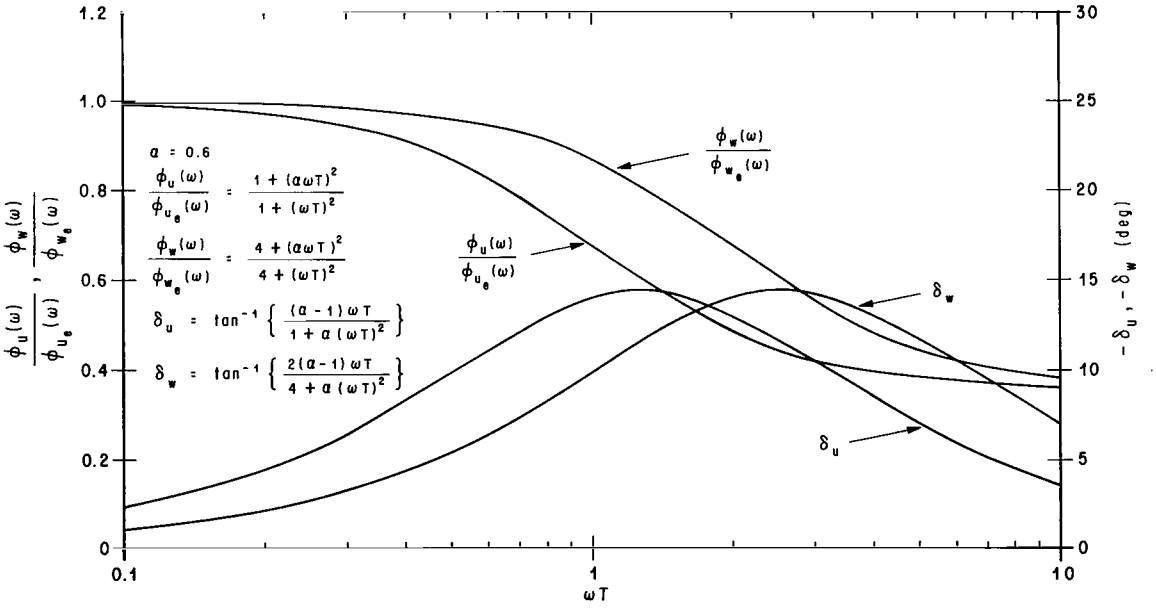

Figure 3. System transfer functions and phase angles as functions of ωT for $a = 0.6$.

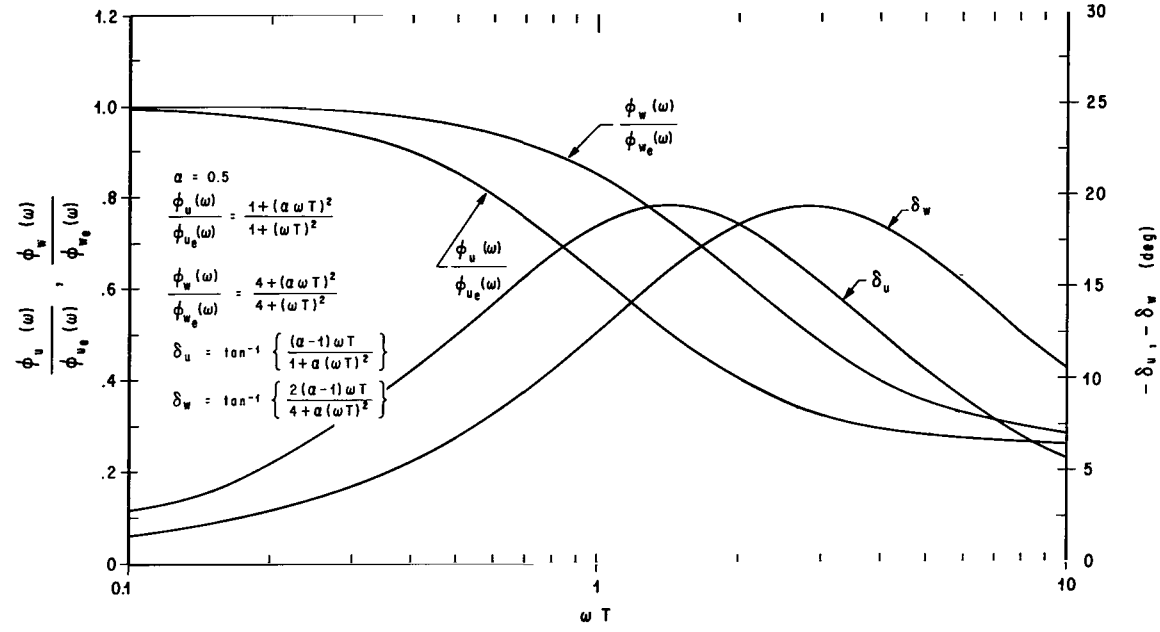

Figure 4. System transfer functions and phase angles as functions of ωT for $\alpha = 0.5$.

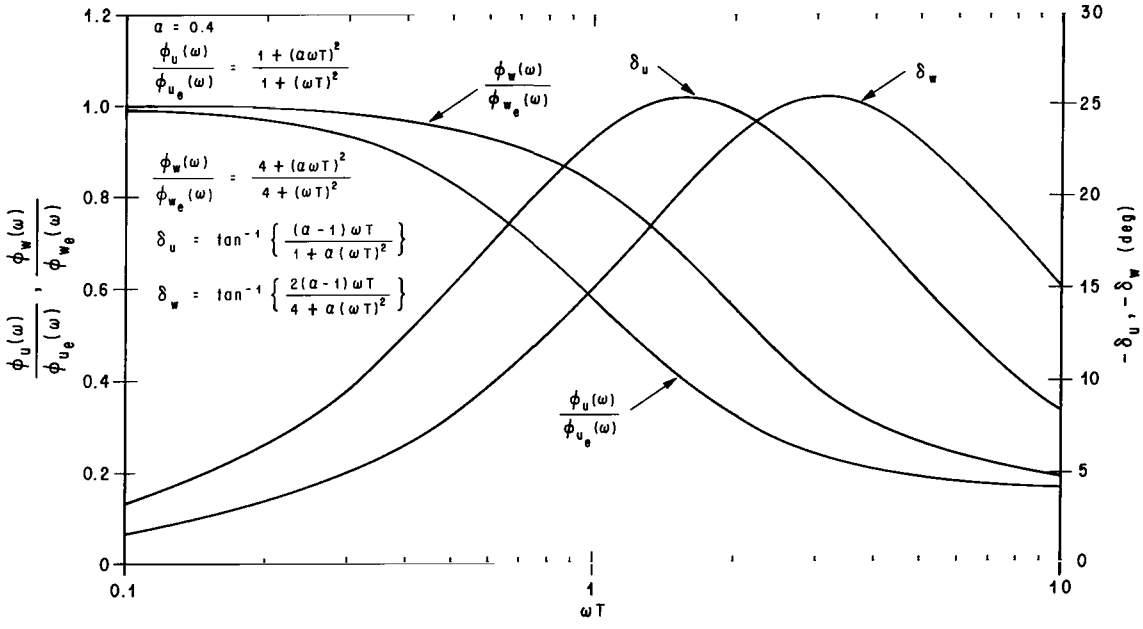

Figure 5. System transfer functions and phase angles as functions of ωT for $\alpha = 0.4$.

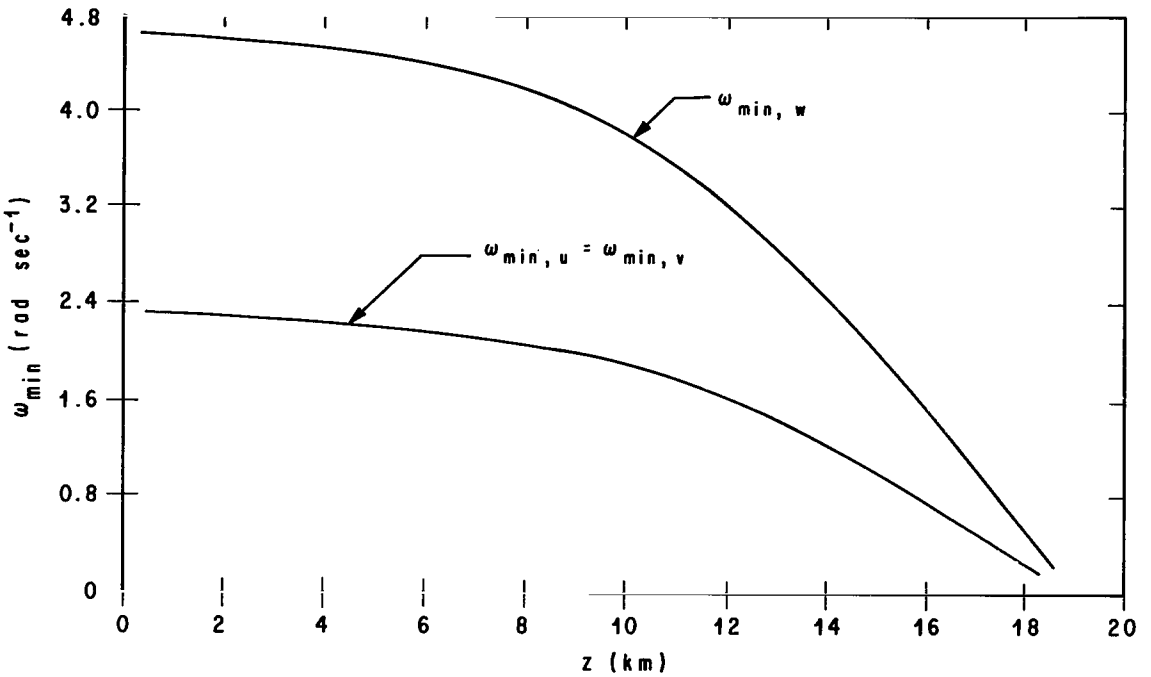

Figure 6. The frequencies $\omega_{min, u}$, $\omega_{min, v}$, and $\omega_{min, w}$ at which the minimum phase angles occur for the Jimsphere wind sensor as functions of altitude.

It is clear from Figures 2 through 5 that the transfer functions approach a^2 as $\omega T \to \infty$. In fact, the response functions essentially assume constant values at $\omega T = 2\pi$, especially for the horizontal velocity fluctuations.

The transfer functions are increasing functions of a and decreasing functions of T. In view of the fact that the quantities a and T are monotonically decreasing and increasing functions of height, respectively, it follows that the transfer functions are decreasing functions of height for any particular value of ω. In short, the Jimsphere becomes less responsive as height increases. An examination of Figures 2 through 5 will show that this is indeed the case.

POWER SPECTRA

As the wind sensor ascends or descends through the atmosphere, it will be carried with the horizontal mean wind. This means the sensor is probing the atmosphere vertically relative to a coordinate system moving with the mean wind. Thus, the environmental

vertical velocity spectrum of the wind fluctuations along the sensor track relative to the environmental mean flow is a longitudinal spectrum. Similarly, the zonal and meridional velocity spectra of the wind fluctuations along the sensor track relative to the mean environmental flow are lateral spectra. These statements are true only if the mean wind is independent of height. In the analysis that follows, it is assumed that environmental fluctuations are isotropic. According to Batchelor [10], the longitudinal and lateral spectra in wave number space are related through the equation,

$$\Phi_{u_e}(\kappa) = \frac{1}{2}\left[\Phi_{w_e}(\kappa) - \kappa \frac{\partial \Phi_{w_e}(\kappa)}{\partial \kappa}\right] \quad , \tag{50}$$

where $\Phi_{w_e}(\kappa)$ and $\Phi_{u_e}(\kappa)$ denote the longitudinal and lateral spectra of the wind fluctuations along the balloon track relative to the mean environmental flow and κ is a vertical wave number ($2\pi/\lambda$, λ being a wavelength). One can convert wave number spectra to frequency spectra with a Jacobian transformation and Taylor's hypothesis which states that

$$\omega = \kappa \bar{w} \quad . \tag{51}$$

The Jacobian transformation is energy perserving and states that

$$\phi(\omega) = \Phi(\kappa) \frac{d\kappa}{d\omega} \quad , \tag{52}$$

where ϕ and Φ denote frequency and wave number spectra. Substitution of equation (51) into equation (52) yields the result

$$\phi(\omega) = \frac{1}{\bar{w}} \Phi\left(\frac{\omega}{\bar{w}}\right) \quad . \tag{53}$$

Substitution of this result into equation (50) yields

$$\phi_{u_e}(\omega) = \frac{1}{2}\left[\phi_{w_e}(\omega) - \omega \frac{\partial \phi_{w_e}}{\partial \omega}\right] \tag{54}$$

In the case of isotropic turbulence $\phi_{u_e} = \phi_{v_e}$, so that all comments that follow relative to ϕ_{u_e} are equally valid for ϕ_{v_e}.

Many types of random wind phenomena have spectra that behave as does

$$\Phi_{w_e}(\kappa) = \beta\kappa^p \quad , \tag{55}$$

where p is a constant and β depends on the intensity of the phenomena. In the case of isotropic turbulence associated with the inertial subrange, $p = -5/3$ and

$$\beta = a_1 \frac{9}{55} \epsilon^{2/3} \quad , \tag{56}$$

where ϵ is the viscous dissipation and a_1 is a universal constant with numerical value approximately equal to 1.4 [11]. In the case of nearly inertial isotropic turbulence with sufficiently small wave numbers in a stably stratified fluid, $p = -3$ and

$$\beta = \frac{Ca_1}{2} \frac{2}{T_o} \frac{\partial \bar{\theta}}{\partial z} \quad , \tag{57}$$

where C is a universal constant, g is the acceleration of gravity, T_o is the temperature of an adiabatic atmosphere, and $\bar{\theta}$ denotes the local mean flow potential temperature [12].

Combining equations (51), (53), (54), and (55) yields

$$\psi_{u_e}(\omega T) = \frac{T^p \bar{w}^{1+p}}{\beta} \phi_{u_e}(\omega) = \frac{1-p}{2} (\omega T)^p \tag{58}$$

and

$$\psi_{w_e}(\omega T) = \frac{T^p \bar{w}^{1+p}}{\beta} \phi_{w_e}(\omega) = (\omega T)^p \quad , \tag{59}$$

where multiplication of the spectra with $T^p \bar{w}^{1+p} \beta^{-1}$ results in the nondimensional quantity $\psi(\omega T)$. Multiplication of equations (58) and (59) by the transfer functions (37) and (38) yields the nondimensional velocity spectra of the sensor; namely,

$$\psi_u = \psi_v = \frac{1-p}{2} \left[\frac{1 + (a\omega T)^2}{1 + (\omega T)^2} \right] (\omega T)^p \tag{60}$$

and

$$\psi_w = \frac{4 + (a\omega T)^2}{4 + (\omega T)^2} (\omega T)^p \quad . \tag{61}$$

In the case of the inertial subrange, one has

$$\psi_u = \frac{4}{3} \left[\frac{1 + (a\omega T)^2}{1 + (\omega T)^2} \right] (\omega T)^{-5/3} \tag{62}$$

and

$$\psi_w = \left[\frac{4 + (a\omega T)^2}{4 + (\omega T)^2} \right] (\omega T)^{-5/3} \quad . \tag{63}$$

For nearly inertial isotropic turbulence in a stably stratified fluid, one has

$$\psi_u = 2 \left[\frac{1 + (a\omega T)^2}{1 + (\omega T)^2} \right] (\omega T)^{-3} \tag{64}$$

and

$$\psi_w = \left[\frac{4 + (a\omega T)^2}{4 + (\omega T)^2} \right] (\omega T)^{-3} \quad . \tag{65}$$

As $\omega T \to \infty$, the asymptotic behavior is obtained

$$\psi_u \sim \frac{1-p}{2} a^2 (\omega T)^p \tag{66}$$

and

$$\psi_w \sim a^2 (\omega T)^p \quad . \tag{67}$$

Thus, at sufficiently large values of ωT, the system transfer functions merely have the effect of reducing the input environmental velocity spectra by a factor a^2 to produce the sensor velocity spectra. This result is a consequence of the apparent mass terms in the equations of motion. If the apparent mass terms were not present in the equations, then ψ_w and ψ_u would approach zero as does $(\omega T)^{p-2}$ as ωT becomes large $(p < 0)$. As $\omega T \to \infty$, the asymptotic behavior is obtained,

$$\psi_u \sim (\omega T)^p \tag{68}$$

and

$$\psi_w \sim (\omega T)^p \quad . \tag{69}$$

Thus, for sufficiently small values of ωT, the system transfer functions have no effect on the input Fourier amplitudes, and the sensor can thus sense virtually 100 percent of the spectral energy.

Figures 7 and 8 contain plots of the input and output nondimensional velocity spectra for turbulence in the inertial subrange and nearly inertial isotropic tubulence in stably stratified air for $a = 0.5$. This value of a occurs at the 13-km level for the Jimsphere balloon (Fig. 1). This region of the atmosphere is notoriously well known for relatively high rates of occurrence of clear air turbulence.

At 13 km, $T = 1.0$ sec and $\bar{w} \simeq 5$ m sec^{-1}, so that $\omega T = 0.63$ corresponds to $\lambda = 50$ m. This wavelength corresponds to the absolute lower limit on the wavelengths of the Fourier components which are not smoothed out by currently available wind profile data reduction procedures [7]. At $\omega T = 0.63$, the system detects 93 percent and 78 percent of the vertical and horizontal wind spectral energies (Fig. 4). However, Figures 7

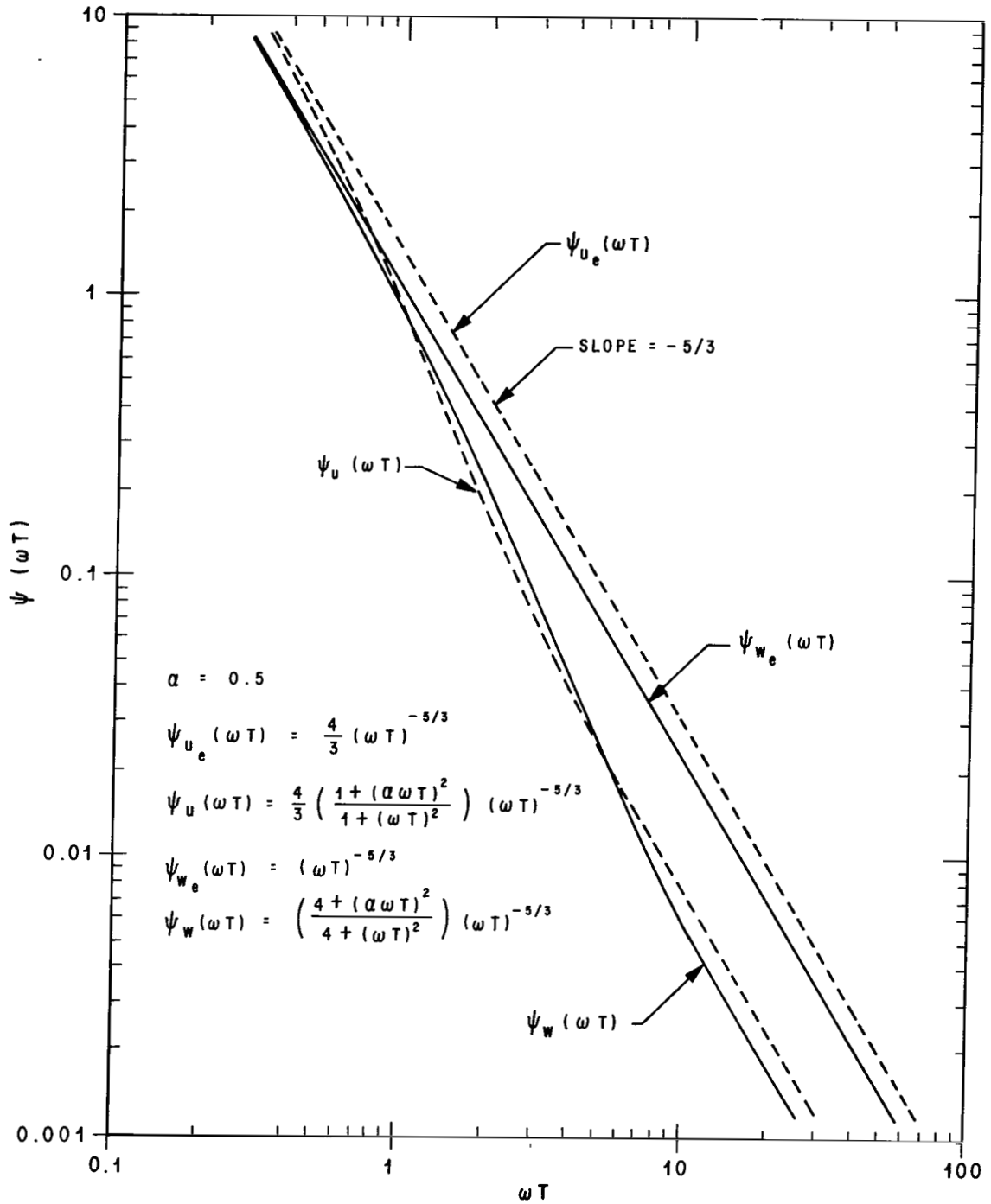

Figure 7. Input and output nondimensional velocity spectra for turbulence in the Kolmogorov inertial subrange as functions of ωT for $\alpha = 0.5$.

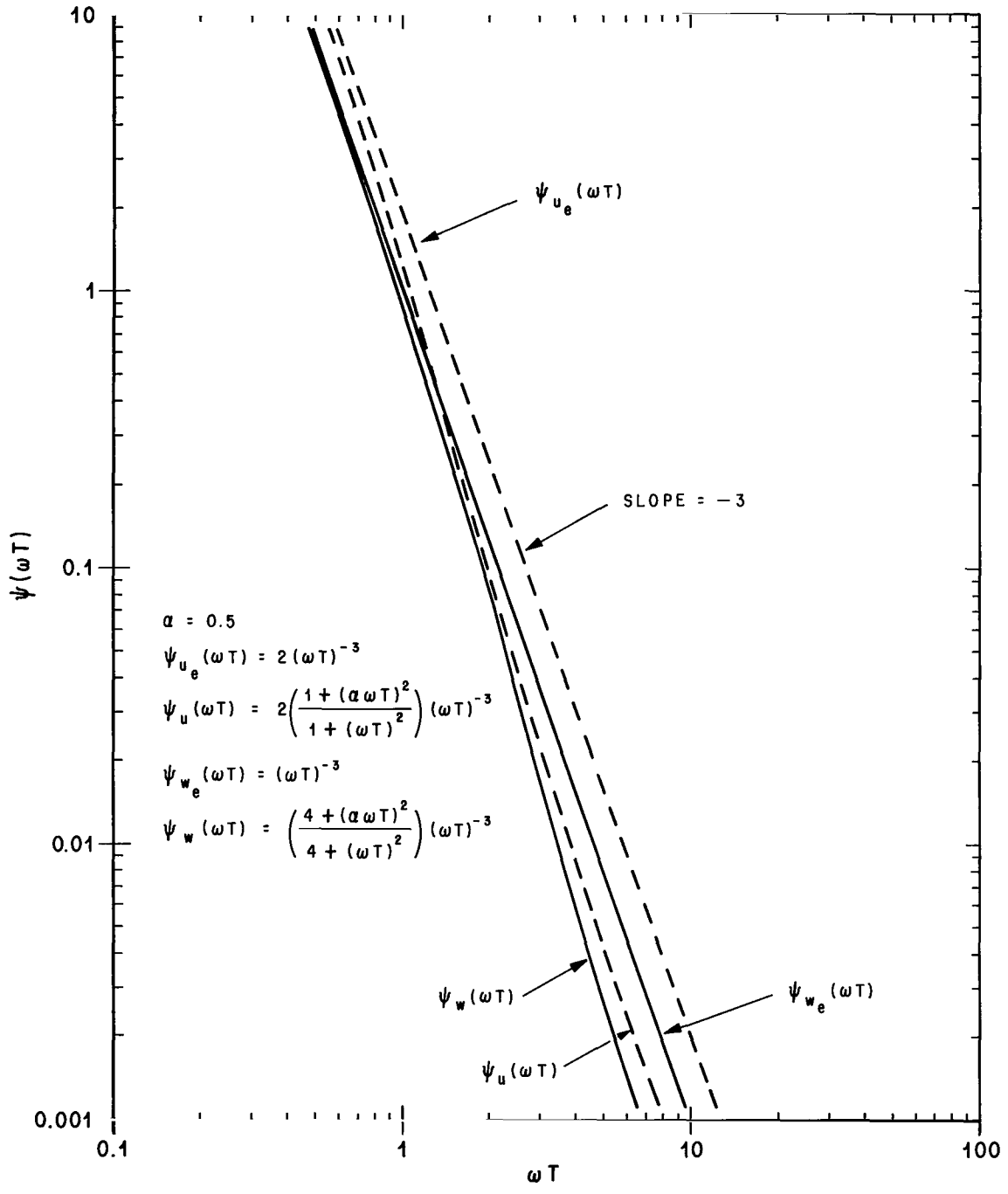

Figure 8. Input and output nondimensional velocity spectra for turbulence in the Lumley subrange as functions of ωT for $a = 0.5$.

and 8 show that there are relatively large amounts of power in the vertical and horizontal sensor spectra at values of $\omega T > 0.63$, especially for the vertical spectra. For example, at $\omega T = 3$ ($\lambda \simeq 10$ m), the sensor vertical velocity spectrum is equal to 48 percent of the corresponding environmental spectrum. To retrieve this information, new and more powerful data reduction procedures of radar wind sensor tracks must be developed.

Figures 7 and 8 clearly show the asymptotic behaviors given by equations (66) through (69) for large and small values of ωT. In the region $0.7 \ \omega T < 6$, the system transfer functions produce output spectra with slopes that are smaller than the input spectra. Thus, in Figure 7 the environmental and balloon spectra have -5/3 and -5/2 slopes, and in Figure 8 the corresponding slopes are -3 and -4 in the domain $0.7 < \omega T < 6$. Thus, if wind profile data are to be analyzed with a view toward detecting clear air turbulence or short wavelength gravity waves in the region $\omega T \gtrsim 1$, then careful attention must be paid to the response properties of the sensor.

CONCLUDING COMMENTS

The response properties of balloon and falling sphere wind sensors in random and turbulent flows have been analyzed. The analysis was based on linearized equations of motion of a wind sensor subject to drag and buoyancy forces. Apparent mass effects have been included, and aerodynamic lift forces have been excluded. It is well known that smooth balloon and falling sphere wind sensors execute lateral self-induced motions resulting from aerodynamic lift forces. The nature of these lateral motions is characterized by the Reynolds number,

$$\mathrm{Re} = \frac{\overline{|w|}\, D}{\nu} \quad , \tag{70}$$

where D is the diameter of the sensor and ν is the coefficient of kinematic viscosity of air. At subcritical Reynolds numbers, for example $\mathrm{Re} \leqslant 2.5 \times 10^5$, smooth spherical wind sensors execute an orderly spiral motion with the vertical wavelength equal to approximately 12 sensor diameters. These motions constitute a very narrow band process, and for all practical purposes, the spectra of the self-induced motions can be represented with Dirac delta functions. At supercritical Reynolds numbers, $\mathrm{Re} > 2.5 \times 10^5$, the self-induced lateral sensor motions resulting from the unstable wake are erratic in nature and occur over a band of frequencies that is broader than the subcritical one. Scoggins [1] finds that the addition of approximately 400 conical roughness elements and a point mass of 100 gm to a smooth 2-m diameter balloon essentially eliminates the erratic character of the self-induced sensor motion at supercritical Reynolds numbers, and causes the balloon to execute an orderly narrow band spiral motion or oscillation at both subcritical and supercritical Reynolds numbers with vertical wavelength equal to approximately 24 m.

It is clear that the analysis in this report is not valid at those frequencies where aerodynamic lift forces are important. Thus, for example, in the case of the Jimsphere balloon, the analysis herein fails at and in a small neighborhood of frequencies about $\omega = 1.3$ rad sec^{-1} ($\lambda = 24$ m and $\bar{w} = 5$ m sec^{-1}) for both subcritical and supercritical Reynolds numbers. The effects of aerodynamic lift forces on balloon and spherical wind sensors will be considered in a later report.

In the analysis, the effects of radar response in the detection of winds with balloons and falling spheres have also been neglected. DeMandel [13] finds that radar errors in wind estimates made with the Jimsphere are concentrated in the horizontal and vertical velocity Fourier components with wavelengths smaller than approximately 100 m and 200 m, respectively. He also points out that the Fourier components of the radar errors and the wind at these wavelengths are of the same order of magnitude. These effects are indeed important, but are not within the scope of the present report. Nevertheless, the problem of determining the joint response of wind sensors and the tracking radar should be examined in the future.

George C. Marshall Space Flight Center
National Aeronautics and Space Administration
Marshall Space Flight Center, Alabama, September 2, 1970
126-61-10-00-62

REFERENCES

1. Scoggins, J. R.: Sphere Behavior and the Measurement of Wind Profiles. NASA TN D-3994, National Aeronautics and Space Administration, 1967.

2. Brockman, W. E.: Small Scale Wind Shears from ROSE Balloon Tracked by AN/FPS-16 Radar. Final Report, AF 19(604)-7450, University of Dayton, 1964.

3. Engler, N. A.: Development of Methods to Determine Winds, Density, Pressure, and Temperature from the ROBIN Falling Balloon. Final Report, AF 19(604)-7450, University of Dayton, 1965.

4. Reed, Wilmer H., III: Dynamic Response of Rising and Falling Balloon Wind Sensors with Application to Estimates of Wind Loads on Launch Vehicles. NASA TN D-1821, National Aeronautics and Space Administration, 1963.

5. Eckstrom, C. V.: Theoretical Study and Engineering Development of Jimsphere Wind Sensor. Final Report, NAS8-11158, G. T. Schjeldahl Co., 1965.

6. Leurs, J.; and Engler, N: On Optimum Methods for Obtaining Wind Data from Balloon Sensors. J. Appl. Meteor., vol. 6, 1967, pp. 816-823.

7. Zartarian, G.; and Thompson, J. H.: Validity of Detailed Balloon Soundings in Booster Vehicle Design. Scientific Report No. 1, AFCRL-68-0606, Kaman Avidyne, 1968.

8. DeMandel, R.; and Krivo, S.: Capability of FPS-16/Jimsphere System for Direct Measurement of Vertical Air Motions. NASA CR-61232, National Aeronautics and Space Administration, 1968.

9. Lumley, J.; and Panofsky, H. A.: The Structure of Atmospheric Turbulence. Interscience Publishers, John Wiley & Sons, New York, 1964.

10. Batchelor, G. K.: The Theory of Homogeneous Turbulence. The University Press, Cambridge, England, 1960.

11. Grant, H. L.; Stewart, R. W.; and Moilliet, A.: Turbulence Spectra from a Tidal Channel. J. Fluid Mech., vol. 12, part 2, 1962, pp. 241-263.

12. Lumley, J. L.: The Spectrum of Nearly Inertial Turbulence in a Stably Stratified Fluid. J. Atmos. Sci., vol. 21, 1964, pp. 99-102.

13. DeMandel, R.: Optimum Filters for Deriving Winds from FPS-16 Radar/Jimsphere Measurements. Preprints of Papers Presented at the Fourth National Conference on Aerospace Meteorology, May 4-7, 1970, Las Vegas, Nev., pp. 136-143.

NASA-Langley, 1971 — 20 M166

01U 001 38 51 3DS 71028 00903
AIR FORCE WEAPONS LABORATORY /WLOL/
KIRTLAND AFB, NEW MEXICO 87117

ATT E. LOU BOWMAN, CHIEF,TECH. LIBRARY

"The aeronautical and space activities of the United States shall be conducted so as to contribute . . . to the expansion of human knowledge of phenomena in the atmosphere and space. The Administration shall provide for the widest practicable and appropriate dissemination of information concerning its activities and the results thereof."

— NATIONAL AERONAUTICS AND SPACE ACT OF 1958

NASA SCIENTIFIC AND TECHNICAL PUBLICATIONS

TECHNICAL REPORTS: Scientific and technical information considered important, complete, and a lasting contribution to existing knowledge.

TECHNICAL NOTES: Information less broad in scope but nevertheless of importance as a contribution to existing knowledge.

TECHNICAL MEMORANDUMS: Information receiving limited distribution because of preliminary data, security classification, or other reasons.

CONTRACTOR REPORTS: Scientific and technical information generated under a NASA contract or grant and considered an important contribution to existing knowledge.

TECHNICAL TRANSLATIONS: Information published in a foreign language considered to merit NASA distribution in English.

SPECIAL PUBLICATIONS: Information derived from or of value to NASA activities. Publications include conference proceedings, monographs, data compilations, handbooks, sourcebooks, and special bibliographies.

TECHNOLOGY UTILIZATION PUBLICATIONS: Information on technology used by NASA that may be of particular interest in commercial and other non-aerospace applications. Publications include Tech Briefs, Technology Utilization Reports and Technology Surveys.

Details on the availability of these publications may be obtained from:

SCIENTIFIC AND TECHNICAL INFORMATION OFFICE

NATIONAL AERONAUTICS AND SPACE ADMINISTRATION

Washington, D.C. 20546